ScientificScholar®
Knowledge is power
Publisher of Scientific Journals

www.surgicalneurologyint.com

Surgical Neurology International

Editor-in-Chief: Nancy E. Epstein, MD, Clinical Professor of Neurological Surgery, School of Medicine, State U. of NY at Stony Brook.

SNI: Neurovascular

Editor
Kazuhiro Hongo, MD
Shinshu University, Matsumoto, Japan

SNI
Open Access

Original Article

Comparison between ultra-high-resolution computed tomographic angiography and conventional computed tomographic angiography in the visualization of the subcallosal artery

Yoshimichi Sato[1], Toshiki Endo[1,2], Shingo Kayano[3], Hitoshi Nemoto[3], Kazuki Shimada[3], Akira Ito[1], Hidenori Endo[1], Shunji Mugikura[4], Kuniyasu Niizuma[1,2,5], Teiji Tominaga[1]

Departments of [1]Neurosurgery, [2]Neurosurgical Engineering and Translational Neuroscience, [3]Radiological Technology, [4]Diagnostic Radiology, Tohoku University Graduate School of Medicine, [5]Department of Neurosurgical Engineering and Translational Neuroscience, Tohoku University Graduate School of Biomedical Engineering, Sendai, Miyagi, Japan.

E-mail: Yoshimichi Sato - yoshimichi4431@nsg.med.tohoku.ac.jp; *Toshiki Endo - endo@nsg.med.tohoku.ac.jp; Shingo Kayano - s_kayano@med.tohoku.ac.jp; Hitoshi Nemoto - h-nemoto@rad.hosp.tohoku.ac.jp; Kazuki Shimada - kazuki.shimada.b7@tohoku.ac.jp; Akira Ito - itoakira0304@gmail.com; Hidenori Endo - h-endo@nsg.med.tohoku.ac.jp; Shunji Mugikura - mugi@rad.med.tohoku.ac.jp; Kuniyasu Niizuma - niizuma@nsg.med.tohoku.ac.jp; Teiji Tominaga - tomi@nsg.med.tohoku.ac.jp

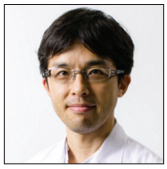

***Corresponding author:**
Toshiki Endo,
Department of Neurosurgery, Tohoku University Graduate School of Medicine, Sendai, Miyagi, Japan.
endo@nsg.med.tohoku.ac.jp

Received : 02 September 2021
Accepted : 26 September 2021
Published : 19 October 2021

DOI
10.25259/SNI_887_2021

Quick Response Code:

ABSTRACT

Background: The subcallosal artery (ScA) is a single dominant artery arising from the anterior communicating artery. Its injury causes amnesia and cognitive disturbance. The conventional computed tomographic angiography (C-CTA) is a common evaluation method of the intracranial artery. However, to image tinny perforating arteries such as the ScA is technically demanding for C-CTA. The purpose of this study is to investigate whether the ultra-high-resolution CTA (UHR-CTA) could image the ScA better than C-CTA. UHR-CTA became available in clinical practice in 2017. Its novel features are the improvement of the detector system and a small X-ray focus.

Methods: Between April 2019 and May 2020, 77 and 49 patients who underwent intracranial UHR-CTA and C-CTA, respectively, were enrolled in this study. Two board-certified neurosurgeons participated as observers to identify the ScA based on UHR-CTA and C-CTA images.

Results: UHR-CTA and C-CTA detected the ScA in 56–58% and 30–40% of the patients, respectively. In visualization of the ScA, UHR-CTA was better than C-CTA ($P < 0.05$, Fisher's exact test). Between the two observers, the Cohen's kappa coefficient was 0.77 for UHR-CTA and 0.78 for C-CTA.

Conclusions: UHR-CTA is a simple and accessible method to evaluate intracranial vasculature. Visualization of the ScA with UHR-CTA was better than that with C-CTA. The high quality of UHR-CTA could provide useful information in the neurosurgery field.

Keywords: Anterior communicating artery, Conventional detector computed tomographic angiography, Subcallosal artery, Ultra-high-resolution computed tomographic angiography

INTRODUCTION

In the surgical treatments for the anterior communicating artery (ACoA) aneurysms or the parachiasmatic tumors, patients may suffer amnesia and cognitive disturbance in after the surgery.[16]

Perforating arteries arising from the ACoA are responsible for these neurological deficits. Yasargil *et al*. named these perforating arteries as hypothalamic arteries in 1984.[23] Later, Marinković *et al*., performed the cadaveric studies to classify them as large and small branches.[7] Serizawa *et al*., focused vascular territories of the perforating arteries and classified them into the three groups including the subcallosal, hypothalamic, and chiasmatic branches.[18] The subcallosal artery (ScA) is a single dominant artery arising from the posterior/posterosuperior surface of the ACoA.[18] It courses posteriorly towards the lamina terminalis region, curving superiorly to the subcallosal area.[2,5,7] The ScA also has a variant with a longer trajectory: The median callosal artery (MdCA).[7] Both the ScA and the MdCA supply the septal/subcallosal region.[7,11] Their injuries are the major cause of amnesia and cognitive disturbance.[10-12] Therefore, accurate assessment of variations and structures of the ScA and the MdCA is particularly important to avoid postoperative complications.

The common evaluation method of the intracranial artery is conventional computed tomographic angiography (C-CTA). However, a diameter of the ScA was 0.5 ± 0.1 mm or lesser, which is technically demanding for C-CTA to visualize.[15]

In 2017, the ultra-high-resolution CTA (UHR-CTA) newly became available in clinical practice. The latest UHR-CTA (Aquilion Precision™; Canon Medical Systems, Tokyo, Japan) provides slice collimation of 0.25 × 160 mm and a matrix size of 1024 × 1024 mm or 2048 × 2048 mm. Its features include an improved detector system and a smaller X-ray focus.[4,22] The detector width is 0.25-mm, which can provide twice the resolution when compared to C-CTA. Several reports indicated that UHR-CT could obtain a high image quality of the intracranial artery.[13,14] In this paper, we investigated whether UHR-CTA could image the ScA and the MdCA better than C-CTA could.

MATERIALS AND METHODS

Patients

From our medical records, we retrospectively retrieved the data of 115 patients who underwent intracranial UHR-CTA and 94 patients who underwent intracranial C-CTA, between April 2019 and May 2020. There were no overlaps between the two groups. We excluded 38 and 45 patients who underwent intracranial UHR-CTA and intracranial C-CTA, respectively, for the following reasons: unavailable datasets, scanning parameters different from those defined in the protocol, and tumors near the ScA. Therefore, 77 patients who underwent intracranial UHR-CTA (37 men and 40 women; age range, 14–74 years; mean age, 51.6 years) and 49 patients who underwent intracranial C-CTA (20 men and 29 women; age range, 3–82 years; mean age, 48.7 years) were enrolled in this study. In the enrolled cases, we included 4 patients who underwent the clipping surgery of the ACoA aneurysms. Three and one patients underwent UHR-CTA and C-CTA, respectively. This study was approved by the Ethical Review Board of Tohoku University Hospital (2020-1-413). We obtained written informed consent from all the patients regarding CTA examinations. For this retrospective study, our ethical review board did not require written informed consents from each individual regarding the participation of this study. The clinical characteristics of the patients enrolled in this study are summarized in [Table 1].

CTA protocols

UHR-CTA was performed using a 160-detector row UHR-CT scanner system. The helical scanning parameters were as follows: tube voltage = 120 kV, tube current = 240 mA, collimation = 0.25 mm × 160, beam pitch factor = 0.569, rotation speed = 0.75 s, slice thickness = 0.25 mm, slice interval = 0.25 mm, scan coverage = 160 mm, reconstruction kernel = forward-projected model-based iterative reconstruction solution algorithm by Canon Medical Systems, and scanning field of view (FOV) = 320 mm. The scan coverage was set for whole brain, with 1024 × 1024 matrix, and display FOV of 200–220 mm. The mean CT dose index volume ($CTDI_{vol}$) and dose-length product (DLP) were 41.7 mGy and 879.4 mGy cm, respectively.

C-CTA studies were performed using a 320-detector row CT system (Aquilion ONE Vision; Canon Medical Systems,

Table 1: Clinical characteristics of patients enrolled in this study.

	UHR-CTA (*n*=77)	C-CTA (*n*=49)
Age (years); mean (range)	51.6 (14–74)	48.7 (3–82)
Women: Men (%Women)	40:37 (51)	29:20 (59)
Disease *n* (%)		
Aneurysm	24 (31) *	17 (34) **
Acoustic tumor	2 (3)	1 (2)
Dural AVF	1 (1)	0 (0)
AVM	0 (0)	1 (2)
Epidermoid cyst	1 (1)	0 (0)
Facial spasm	2 (3)	1 (2)
Metastatic tumor	0 (0)	2 (4)
Cavernoma	1 (1)	0 (0)
Glioma	5 (7)	5 (10)
Hemangioblastoma	3 (4)	2 (4)
Teratoma	1 (1)	0 (0)
Meningioma	23 (31)	7 (15)
Epilepsy	10 (14)	7 (15)
Intracranial artery stenosis	0 (0)	4 (8)
Others	4 (5)	2 (4)

UHR–CTA: Ultra-high-resolution computed tomography angiography, C-CTA: Conventional computed tomography angiography, *Three aneurysms located in the anterior communicating artery. **One aneurysm located in the anterior communicating artery

Otawara, Japan). The volume scanning parameters were as follows: tube voltage = 120 kV, automatic exposure control tube current standard deviation = 7, collimation = 0.5 mm × 320, rotation speed = 1.5 s, slice thickness = 0.5 mm; slice interval = 0.25 mm, scan coverage = 160 mm, reconstruction kernel = FC44, iterative and noise-reduction filters = adaptive iterative dose reduction algorithm by Canon Medical Systems, and scanning FOV = 240 mm. The scan coverage was set for the whole brain, with a display FOV of 200–220 mm. The mean $CTDI_{vol}$ and mean DLP were 54.29 ± 9.1 mGy and 866.6 ± 144.5 mGy cm, respectively.

Nonionic contrast medium with an iodine concentration between 300 and 370 mgI/mL was used selectively according to body weight (iomeprol [Iomeron300; Eisai Co., Ltd., Tokyo, Japan], ioversol [Optiray320; Guerbet Japan Co., Ltd., Tokyo, Japan], iohexol [OMNIPAQUE350; GE Healthcare Pharma Co., Ltd., Tokyo, Japan], and iopamidol [Iopamiron370; Bayer Yakuhin, Ltd., Osaka, Japan]). Contrast medium was delivered via a 20-gauge catheter inserted into the antecubital vein with an injection flow rate based on the patient's body weight in kilograms (main bolus injection: UHR-CTA, 27.5 mgI/kg/s; C-CTA, 26 mgI/kg/s). The injection time was 12 s for C-CTA and 14 s for UHR-CTA.

Image postprocessing and data analysis

To evaluate the ScA and the MdCA, sagittal maximum intensity projection (MIP) images with 2 mm thickness were reconstructed from UHR-CTA and C-CTA images. These MIP images were generated using a commercially available workstation (Ziostation2; Ziosoft, Tokyo, Japan). Patients with a surgical clip were evaluated with the same method. The ScA was defined as an artery arising from the posterior/posterosuperior surface of the ACoA and running to the pericallosal cistern but not extending beyond the genu of the corpus callosum.[15] When we found the artery extending beyond the genu and supplying the medial hemispheric surface, we named it as the MdCA and counted separately.[7]

Statistical analysis

From the generated UHR-CTA and C-CTA images, the ScA and the MdCA were visually assessed. Two independent experienced neurosurgeons (YS and TE) participated as observers. The concordance between the two observers was evaluated based on Cohen's kappa coefficient interpreted as follows: ≤0, no agreement; 0.01–0.20, none to slight agreement; 0.21–0.40, fair agreement; 0.41–0.60, moderate agreement; 0.61–0.80, substantial agreement; and 0.81–1.00, almost perfect agreement.[3] Fisher's exact *t*-test was used to calculate the *P*-values of the comparisons. For all statistical analyses, a *P*-value of 0.05 indicated a statistically significant inter-group difference. We conducted this analysis using Statistical Package for the Social Sciences version 24.0.0. software. (IBM, Armonk, NY, USA).

RESULTS

Number of subcallosal arteries recognized in the UHR-CTA and C-CTA images

The first observer (YS) identified the ScA in 45 patients (58%) and 15 patients (30%) on the UHR-CTA and C-CTA images, respectively. The second observer (TE) detected the ScA in 43 patients (56%) and 18 patients (40%) on the UHR-CTA and C-CTA images, respectively. Both of the two observers identified the MdCA in 3 (3.9%) and 1 case (2.3%) in UHR-CTA and C-CTA, respectively.

Regarding the ScA, the Cohen's kappa coefficient was 0.77 for UHR-CTA and 0.78 for C-CTA. The average results of the two observers are shown in [Table 2]. Overall, the UHR-CTA was significantly better than C-CTA in recognizing the ScA ($P < 0.05$, Fisher's exact test).

Representative images of the ScA obtained from UHR-CTA and C-CTA are shown in [Figure 1]. UHR-CTA provided clear sagittal MIP images, which aided clinicians to recognize

Table 2: The averaged numbers of the cases that the C-CTA and UHR-CTA recognized the ScA.

	ScA positive	ScA negative
UHR-CTA (*n*=77) (%)	44 (57.1)	33 (42.9)
C-CTA (*n*=49) (%)	16.5 (33.7)	32.5 (66.3)

The *P* value=0.01 by Fisher's exact test, ScA; Subcallosal artery, UHR-CTA; ultra-high-resolution computed tomography angiography, C-CTA; conventional computed tomography angiography

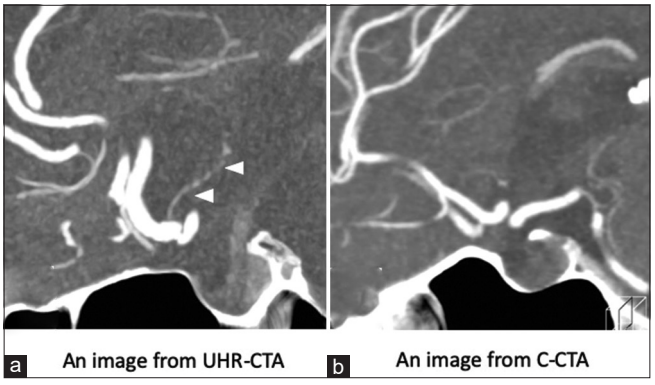

Figure 1: Representative sagittal maximum intensity projection images from ultra-high-resolution computed tomographic angiography (UHR-CTA) (a) and conventional computed tomographic angiography (C-CTA) (b). In UHR-CTA, the higher image quality permitted the identification of the subcallosal artery (ScA) as an artery arising from the posterior surface of the anterior communicating artery (arrowheads in a). While, in C-CTA, the ScA was not identified.

the ScAs [Figure 1]. However, the sagittal MIP image from C-CTA was blurry. In a representative case, the ScA was not identified [Figure 1].

Subcallosal arteries after the ACoA aneurysmal surgery

Among the 4 patients who underwent the clipping surgery for the ACoA aneurysms, UHR-CTA detected the ScA in 2 out of 3 patients (67%) [Figure 2]. C-CTA failed to show the ScA in one patient after the clip was applied to obliterate the ACoA aneurysm (0%).

DISCUSSION

In this study, the ScAs were detected more frequently on UHR-CTA images. The UHR-CTA detected the ScA in 56–58% of the patients, while the C-CTA could detect the ScA only in 30–40% of the patients. The difference was statistically significant. In our analyses, the MdCA were also identified in 2.3% to 3.9% of the cases. According to the cadaveric study by Marinković *et al*., the ScA and the MdCA callosum were complementary,[7] which was in line with our observations.

UHR-CTA

Since cadaver head dissections found the ScAs in 80% of the specimens,[7,15] we interpreted that the image quality of the C-CTA was not high enough to visualize a small but important artery, the ScA.[13] However, the emergence of the UHR-CTA scanner has changed the situations.[13,14] The UHR-CTA scanner is equipped with a 0.25-mm detector that enables the scanning of images with half thickness and provides images at a higher resolution. A recent report demonstrated that UHR-CTA and C-CTA detected 2.85 and 2.17 lenticulostriate arteries, respectively.[13] Since there was a significant difference, the UHR-CTA was found to be superior to the C-CTA in visualizing perforating arteries from the middle cerebral arteries.[13] The current study proved that the UHR-CTA could detect perforating arteries from the ACoA better than C-CTA could. This adds further evidence to UHR-CTA being a useful tool in clinical situations.

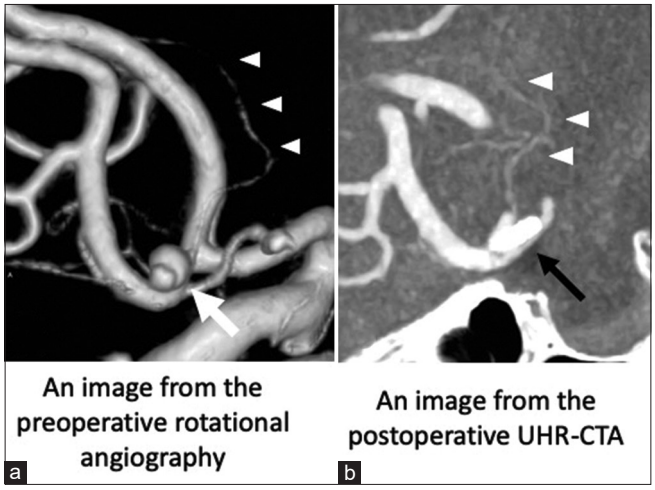

Figure 2: Pre and postoperative images of a 73-year-old woman who underwent the clipping operation for the ruptured anterior communicating artery (ACoA) aneurysm. (a) A three dimensional reconstructed image of the rotational angiography demonstrating ACoA aneurysm (arrow) and the subcallosal artery (ScA, arrowheads). (b) Sagittal maximum intensity projection image of the ultra-high-resolution computed tomographic angiography demonstrate the ScA (arrowheads) even after the clip was applied to the ACoA aneurysm (black arrow).

ScA and ACoA aneurysmal surgery

The visualization and preservation of the ScA have always been an issue in surgical interventions performed for ACoA aneurysms.[12,21] The ScA supplies blood to the bilateral anterior columns of the fornix. Since the fornix is a white matter tract bundle that acts as the major output of the hippocampus, it plays an important role in the formation and consolidation of declarative memories.[19,20] Mortimer *et al*. reported that 31 of 66 (47%) patients showed postoperative infarction after ACoA aneurysmal clippings.[9] Mugikura *et al*., confirmed causative relationship between the ScA infarction and postoperative amnesia.[10]

The current study included four postoperative cases after the clipping surgeries for the ACoA aneurysms. Importantly, the ScA near the surgical clip was successfully imaged in UHR-CTA in 2 out of 3 cases. Our results indicated that the artifacts of the surgical clips were reduced in UHR-CTA when compared to those in C-CTA. To explain the low metallic artifacts in UHR-CTA, two hypotheses including the high effective energy and the high spatial resolution were suggested. As the effective energy rises, the beam hardening artifact from the aneurysm clip reduces.[6] Further, the high spatial resolution can reduce the partial volume artifact from the surgical clips.[1,17] It would be noteworthy if UHR-CTA could provide reliable images to evaluate perforating arteries even after the aneurysmal clipping surgery. This feature would make UHR-CTA an important tool to help neurosurgeons to proceed complex vascular surgical procedures.

Magnetic resonance imaging (MRI) and magnetic resonance angiography (MRA)

MRA can be another option to assess intracranial arteries in a non-invasive manner. It does not require any contrast medium and is less invasive than CTA. However, visualization of a small perforating artery, such as the ScA, has not yet been

successful with 1.5- or 3-Tesla MRAs. Recently, several studies indicated that 7-Tesla MRA could be useful for studying the microanatomy of perforating arteries. Matsushige *et al*. reported that branching arteries originating from the ACoA, including the ScA, were visualized on a 7-Tesla MRI in 85.1% of the participants.[8] However, the 7-Tesla MRA has several issues to resolve, including magnetic field inhomogeneity, patient safety, and high cost, before it can become a routine imaging modality in regular clinics. Under these circumstances, the UHR-CTA could be a feasible and reliable option for evaluating intracranial perforating arteries.

Limitations

In the current protocol, we could not compare images of these two types of CTA in the same individuals, which is major limitation. Another limitation of this study was that we only analyzed the ScA and the MdCA among other various perforating arteries. As Serizawa *et al*., reported, the ACoA perforators included hypothalamic and chiasmatic branches[18] whose diameters ranged from 0.1 to 0.3 mm. Having considered the collimation size of the UHR-CTA was 0.25 mm, we focused on the ScA and the MdCA; the large branch with a diameter around 0.5mm to verify the efficacy of the UHR-CTA.

Furthermore, we could only include the postoperative AcoA aneurysm cases in very limited numbers in this study. The artifacts near the surgical clip might have influenced the image quality of the UHR-CTA; however, this issue was beyond the scope of this study. We are now planning another clinical study to determine whether UHR-CTA could potentially provide high-quality images to evaluate the preservation of the perforating arteries near the surgical clips and whether they could influence surgical results and overall outcomes of the patients.

CONCLUSIONS

UHR-CTA considerably improved the visualization of the ScA. UHR-CT is a simple and easily accessible method to evaluate microvasculature, such as the ScA, especially in the neurosurgery field.

Acknowledgment

We would like to thank Editage (www.editage.com) for English language editing.

Declaration of patient consent

Institutional Review Board (IRB) permission obtained for the study. IRB did not require written informed consents from each individual regarding the participation of this study.

Financial support and sponsorship

This study was supported by JSPS Grant-in-Aid for Scientific Research. No author has personal or institutional financial interest in drugs, materials, or devices described in this paper.

Conflicts of interest

There are no conflicts of interest.

REFERENCES

1. Barrett JF, Keat N. Artifacts in CT: Recognition and avoidance. Radiographics 2004;24:1679-91.
2. Chenin L, Kaoudi A, Foulon P, Havet E, Peltier J. Microsurgical anatomy of the subcallosal artery. Surg Radiol Anat 2019;41:1037-44.
3. Cohen J. A coefficient of agreement for nominal scales. Educ Psychol Meas 1960;20:37-46.
4. Kakinuma R, Moriyama N, Muramatsu Y, Gomi S, Suzuki M, Nagasawa H, *et al*. Ultra-high-resolution computed tomography of the lung: Image quality of a prototype scanner. PLoS One 2015;10:e0137165.
5. Kannath SK, Malik V, Rajan JE. Isolated subcallosal artery infarction secondary to localized cerebral vasospasm of anterior communicating artery complex following subarachnoid hemorrhage. World Neurosurg 2017;107:1043.e15-8.
6. Katsura M, Sato J, Akahane M, Kunimatsu A, Abe O. Current and novel techniques for metal artifact reduction at CT: Practical guide for radiologists. Radiographics 2018;38:450-61.
7. Marinković S, Milisavljević M, Marinković Z. Branches of the anterior communicating artery. Microsurgical anatomy. Acta Neurochir (Wien) 1990;106:78-85.
8. Matsushige T, Chen B, Dammann P, Johst S, Quick HH, Ladd ME, *et al*. Microanatomy of the subcallosal artery: An *in vivo* 7 T magnetic resonance angiography study. Eur Radiol 2016;26:2908-14.
9. Mortimer AM, Steinfort B, Faulder K, Erho T, Scherman DB, Rao PJ, *et al*. Rates of local procedural-related structural injury following clipping or coiling of anterior communicating artery aneurysms. J Neurointerv Surg 2016;8:256-64.
10. Mugikura S, Kikuchi H, Fujii T, Murata T, Takase K, Mori E, *et al*. MR imaging of subcallosal artery infarct causing amnesia after surgery for anterior communicating artery aneurysm. AJNR Am J Neuroradiol 2014;35:2293-301.
11. Mugikura S, Kikuchi H, Fujimura M, Mori E, Takahashi S, Takase K. Subcallosal and Heubner artery infarcts following surgical repair of an anterior communicating artery aneurysm: A causal relationship with postoperative amnesia and long-term outcome. Jpn J Radiol 2018;36:81-9.
12. Mugikura S, Mori N, Kikuchi H, Mori E, Takahashi S, Takase K. Relationship between decreased cerebral blood flow and amnesia after microsurgery for anterior communicating artery aneurysm. Ann Nucl Med 2020;34:220-7.
13. Murayama K, Suzuki S, Nagata H, Oda J, Nakahara I, Katada K, *et al*. Visualization of lenticulostriate arteries on CT angiography using ultra-high-resolution CT compared

with conventional-detector CT. AJNR Am J Neuroradiol 2020;41:219-23.
14. Nagata H, Murayama K, Suzuki S, Watanabe A, Hayakawa M, Saito Y, *et al*. Initial clinical experience of a prototype ultra-high-resolution CT for assessment of small intracranial arteries. Jpn J Radiol 2019;37:283-91.
15. Najera E, Belo JT, Truong HQ, Gardner PA, Fernandez-Miranda JC. Surgical anatomy of the subcallosal artery: Implications for transcranial and endoscopic endonasal surgery in the suprachiasmatic region. Oper Neurosurg (Hagerstown) 2019;17:79-87.
16. Norlen G, Barnum AS. Surgical treatment of aneurysms of the anterior communicating artery. J Neurosurg 1953;10:634-50.
17. Sakai Y, Kitamoto E, Okamura K, Tatsumi M, Shirasaka T, Mikayama R, *et al*. Metal artefact reduction in the oral cavity using deep learning reconstruction algorithm in ultra-high-resolution computed tomography: A phantom study. Dentomaxillofac Radiol 2021;50:20200553.
18. Serizawa T, Saeki N, Yamaura A. Microsurgical anatomy and clinical significance of the anterior communicating artery and its perforating branches. Neurosurgery 1997;40:1211-6; discussion 1216-8.
19. Sutherland RJ, Rodriguez AJ. The role of the fornix/fimbria and some related subcortical structures in place learning and memory. Behav Brain Res 1989;32:265-77.
20. Thomas AG, Koumellis P, Dineen RA. The fornix in health and disease: An imaging review. Radiographics 2011;31:1107-21.
21. Türe U, Yaşargil MG, Krisht AF. The arteries of the corpus callosum: A microsurgical anatomic study. Neurosurgery 1996;39:1075-1084; discussion 1084-5.
22. Yanagawa M, Hata A, Honda O, Kikuchi N, Miyata T, Uranishi A, *et al*. Subjective and objective comparisons of image quality between ultra-high-resolution CT and conventional area detector CT in phantoms and cadaveric human lungs. Eur Radiol 2018;28:5060-8.
23. Yasargil MG, Kasdaglis K, Jain KK, Weber HP. Anatomical observations of the subarachnoid cisterns of the brain during surgery. J Neurosurg 1976;44:298-302.

How to cite this article: Sato Y, Endo T, Kayano S, Nemoto H, Shimada K, Ito A, *et al*. Comparison between ultra-high-resolution computed tomographic angiography and conventional computed tomographic angiography in the visualization of the subcallosal artery. Surg Neurol Int 2021;12:528.